Optical spectra of $Y_{1-x}Ca_xVO_3$: Change of electronic structures with hole doping in Mott-Hubbard insulators

M. Kasuya, Y. Tokura,* and T. Arima
Department of Physics, University of Tokyo, Tokyo 113, Japan

H. Eisaki
Department of Applied Physics, University of Tokyo, Tokyo 113, Japan

S. Uchida
Superconductivity Research Course, University of Tokyo, Tokyo 113, Japan
(Received 10 June 1992)

In perovskitelike solid solutions $Y_{1-x}Ca_xVO_3$, the insulator-metal transition has been observed around $x=0.5$, which can be interpreted as being caused by hole doping in a Mott-Hubbard insulator YVO_3. Change of electronic structures has been investigated by measurements and analyses of optical spectra. New electronic states were observed to grow within the Mott-Hubbard gap upon hole doping and eventually compose the states near the Fermi level in the metallic phase. Doping-induced changes of electronic structures are argued in comparison with the case of cuprate superconductors.

I. INTRODUCTION

Intensive studies on normal-state properties in cuprate superconductors have revealed a number of important features inherent in the strongly electron-correlated systems.[1] In the Zaanen-Sawatzky-Allen scheme,[2] insulating compounds arising from the strong correlation between d electrons can be categorized into either of two classes, Mott insulators (in a narrow sense) or charge-transfer (CT) insulators, according to whether the minimum charge gap is formed between the d-electron states (upper and lower Hubbard bands) or between the ligand (e.g., oxygen) p state and the upper Hubbard band. The parent compounds for cuprate superconductors have been assigned to CT-type insulators, whereas some light transition-metal oxides, e.g., V_2O_3 (Ref. 3), with localized d-electron states are the Mott insulators. There are ample examples of phase transitions due to the collapse of the Mott-Hubbard gap.[4] Recently, the metal-insulator transition associated with an opening of the CT gap has been reported for $RNiO_3$ (R = rare-earth element) when changing the species of R (Ref. 5).

In addition to such a phase change associated with an opening or closing of the Mott-type or CT-type gap at the fixed integer valence of a constituent metal element, there is another type of insulator-metal transition, which is caused by a change in the nominal metal valence (or in the band filling). The latter procedure is sometimes called *carrier doping*, yet the electronic process is qualitatively different from the case of conventional doped semiconductors with weak electron correlation. A typical example of the doping-induced CT insulator-metal (superconductor) transition is that observed in layered cuprate compounds, where drastic changes of electronic structures and properties have been observed with carrier doping. Complementary to those studies, we have tried in the present study to clarify the change in electronic structure occurring with the doping-induced Mott insulator-metal transition in vanadium oxide compounds.

As well exemplified[6] in the cases of hole-doped superconductors $La_{2-x}Sr_xCuO_4$ and electron-doped superconductors $Nd_{2-x}Ce_xCuO_4$, the band filling (or number of $3d$ electrons) can be controlled in the A_rBO_y-type ternary compounds by alloying the A-site cations, e.g., with trivalent rare-earth and divalent alkaline-earth ions, while keeping the essential transition-metal (B-site) oxygen networks. (Here r is the ratio of A-site ions to transition metals (B-site) and y is the oxygen content.) For this purpose, we have chosen for this study perovskitelike ternary oxides ($r=1, y=3$), YVO_3 and their partly Ca-substituted analogs $Y_{1-x}Ca_xVO_3$. Using such a solid solution system, we can continuously control the nominal valence of vanadium from 3+ ($3d^2$) to 4+ ($3d^1$). An analogous solid solution system $La_{1-x}Sr_xVO_3$ (Refs. 7–9) was investigated previously with an interest in the insulator-metal transition. The metal-insulator transition in $La_{1-x}Sr_xVO_3$ was observed around $x=0.2$ with the disappearance of the low-temperature magnetically ordered phase. Recently, the two-dimensional analog, $R_{1-x}Sr_{1+x}VO_4$ (R = rare-earth element) with the K_2NiF_4-type structure, has been investigated with interest in searching for possible superconductivity,[10] yet the system was found to be semiconducting or insulating over the whole composition region ($0 \le x \le 1$). To our knowledge, very little is known about the filling-dependent change in the electronic structure of vanadium oxide systems which may be revealed by various spectroscopic studies. In this paper, we report the spectroscopic investigation of the change in the electronic structure with hole doping in a prototypical Mott insulator, YVO_3. An advantage of using the $Y_{1-x}Ca_xVO_3$ system rather than $La_{1-x}Sr_xVO_3$ is that the former system has a lower (and hence more tractable) melting temperature (1500–1900 °C) (Ref. 11) and it is easier to obtain the

high-quality dense (melt-grown) samples that are suitable for the spectroscopic study.

II. SAMPLE PREPARATION

The samples of $Y_{1-x}Ca_xVO_3$ were melt grown for the compositions from $x=0.0$ to 1.0 at an interval of 0.1. Bar-shaped ingredients were melted in a 7% H_2/Ar atmosphere with the use of a floating zone furnace equipped with two halogen incandescent lamps and hemieliptic focusing mirrors. A traveling speed of the melted zone was set rather high, at $\sim$30 mm/h, to avoid a possible gradient of the composition due to segregation effects. The samples were polycrystalline, but no apparent grain boundary was discernible by visual inspection under an optical microscope. The mechanically polished surfaces were highly specular and showed sufficient quality for optical measurements.

The solid solutions show the $GdFeO_3$-type structure over the whole composition range. The lattice structure can be viewed as an orthorhombically distorted perovskite structure, in which VO_6 octahedra tilt alternatingly[7] as schematically shown in the inset of Fig. 1. The change of lattice parameters with composition was measured by x-ray diffraction of powderized samples, the result of which is shown in Fig. 1. No appreciable difference in lattice parameters has been detected on specimens from different portions of the sample ingot. The lattice parameters show a continuous change with x, ensuring the formation of solid solutions over the entire composition range.

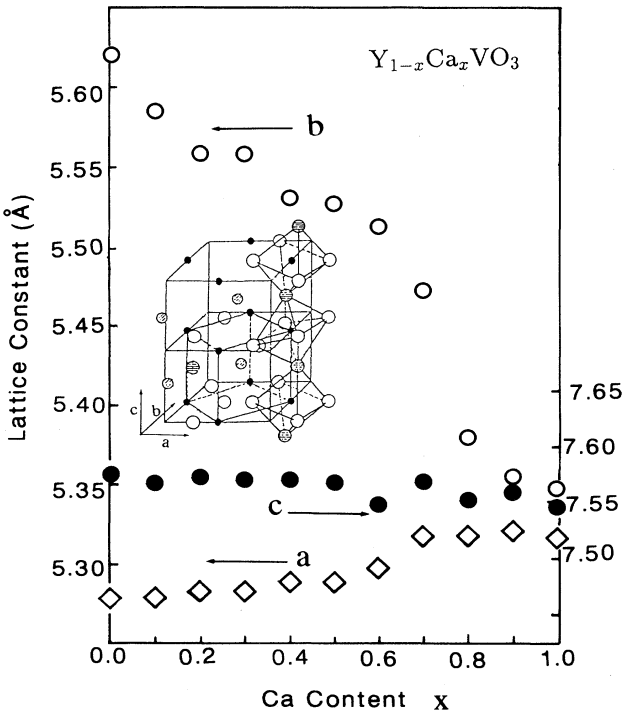

FIG. 1. The change of the lattice constants of the orthorhombic crystals $Y_{1-x}Ca_xVO_3$.

The orthorhombic distortion, as measured by the ratio of the c/a axis length, is decreased with Ca concentration (x). The crystals may show some anisotropic electronic properties due to the orthorhombic distortion. Even in YVO_3 with the maximum orthorhombicity, however, the anisotopy of the interatomic V-V distance is not so significant: 3.80 Å within the lateral direction (ab plane) and 3.85 Å for the c-axis direction. (Note that lengths of the a, b, and c axes in the $GdFeO_3$-type structure are approximately $\sqrt{2}a_p$, $\sqrt{2}a_p$, and $2a_p$, respectively, a_p being the unit-cell length in the cubic perovskite structure. See the inset of Fig. 1.) Within the experimental accuracy that the spectroscopic study can attain, we may consider that the anisotropy is not significant. All the experimental results obtained in the present study were analyzed assuming virtually isotropic electronic and optical properties.

To check possible oxygen nonstoichiometry, we have done thermogravimetric analysis for the compounds. The results indicate that each sample ($Y_{1-x}Ca_xVO_{3-\delta}$) contains oxygen vacancies ($\delta=0.01-0.06$). However, the estimated values were not systematic with x and depended rather on the preparation process of the samples. It should be noted that the oxygen vacancies and resultant change of the d-electron numbers (or vanadium valence) may affect the electronic properties seriously in some cases, in particular for the end compounds, $CaVO_3$ and YVO_3, which would ideally have an integer number (1 or 2) of d electrons per vanadium. The parent compound YVO_3 is well insulating and its electronic properties seem not to be sensitive to a small deviation of vanadium valence. Our aim in the present study is to obtain a perspective on the filling-dependent change of electronic structures in the Mott system, and hence a slight variation of oxygen nonstoichiometry will not be so serious, as far as the present spectroscopic investigation for the insulator-metal trasnsition is concerned.

III. INSULATOR-METAL TRANSITION WITH HOLE DOPING

Measurements of the temperature-dependent resistivity (ρ) were done on the samples of a rectangular shape (cut out from the melted ingot) by the conventional four-probe method with electrodes of indium. The results are shown in Fig. 2 [Note that the ordinate (ρ) is logarithmic in scale.] The compounds with $x=0-0.4$ are typically insulating or semiconducting, showing a behavior of thermally activated conduction with activation energies of $\sim$0.25 eV for $x=0$ and $\sim$0.13 eV for $x=0.1-0.4$ samples. On the other hand, the Ca-rich compounds with $x=0.6-1.0$ show metallic resistivity. Judging from the marginal behavior of the $x=0.5$ sample, it can be concluded that the insulator-metal transition in $Y_{1-x}Ca_xVO_3$ takes place around $x_c=0.5$ According to preliminary measurements, the Hall coefficient (R_H) is negative and small ($\sim -1.5\times10^{-4}$ cm^3/C) for the metallic ($x=0.6$) composition, whereas that in the semiconducting region ($x=0.2$) is positive and very large ($\sim$1.6

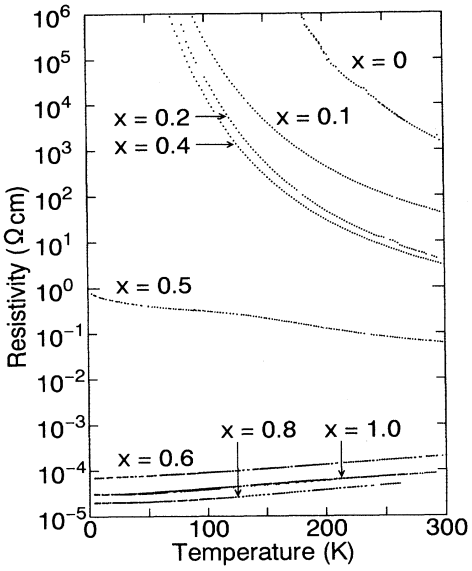

FIG. 2. The temperature dependence of the resistivity in $Y_{1-x}Ca_xVO_3$.

cm^3/C) at room temperature. This indicates that the hole-doping procedure induces the transition from the p-type semiconductor to a metal, but that the metallic phase, at least not too close to the metal-insulator phase boundary ($x_c \sim 0.5$), is characterized by electron-type carriers.

According to measurements of the magnetic susceptibility, YVO_3 was found to undergo a magnetic phase transition around 110 K ($=T_N$), in accord with the results of previous studies.[11,12] The magnetically ordered phase is weakly ferromagnetic, perhaps due to canting of antiferromagnetically coupled spins as in the case of $LaVO_3$ (Refs. 7 and 8). The critical temperature for the magnetic phase transition appears to be suppressed with hole doping and the low-temperature magnetic phase disappears around $x=0.5$, which is in accord with the insulator-metal transition as probed by resistivity measurements (Fig. 2). The overall behavior for the hole-doping-induced insulator-metal transition quite resembles that observed in $La_{1-x}Sr_xVO_3$ (Refs. 7 and 8), though the critical hole concentration necessary for the transition is considerably higher ($x_c \sim 0.5$) in $Y_{1-x}Ca_xVO_3$ than in $La_{1-x}Sr_xVO_3$ ($x_c \sim 0.2$).[7-9] This is perhaps because the $Y_{1-x}Ca_xVO_3$ system shows a larger orthorhombic distortion and, accordingly, a smaller one-electron band width (W) than the $La_{1-x}Sr_xVO_3$ system. The doping-induced insulator-metal transition in real three-dimensional Mott-Hubbard systems takes place after the collapse of the long-range order of the localized spins and the critical hole concentration of such a phase change seems to depend strongly on the strength of the electron correlation (U/W) in the parent Mott insulator, as seen in the present case and also in hole-doped $RTiO_3$ compounds (R = rare-earth element).[13]

IV. CHANGE OF OPTICAL SPECTRA WITH CARRIER DOPING

A. Optical measurements

Reflectivity spectra for $Y_{1-x}Ca_xVO_3$ were measured on specularly polished surfaces of the melt-grown samples at room temperature in the photon energy range from 0.02 to 40 eV. The reflectivity was measured under the condition of nearly normal incidence by Fourier-transform spectroscopy in the infrared region and by grating spectroscopy at higher photon energies. For a light source in the vacuum ultraviolet region (6–40 eV), we utilized synchrotron radiation at INS-SOR, Institute for Solid State Physics, University of Tokyo. The absolute reflectivity was determined by comparison with the known reflectivity of gold film which was measured with the same optical alignment. The reflectance spectra were transformed to the optical conductivity spectra by the Kramers-Kronig relation. For the Kramers-Kronig analysis, the reflectivity data were extrapolated by the Hagen-Rubens approximation $[1-R(\omega) \propto \sqrt{\omega}]$ below 0.05 eV in the metallic phase for $x \geq 0.6$. For the insulating phase for $x \leq 0.4$, the constant reflectivity was assumed below 0.02 eV. For the high-frequency extrapolation above 40 eV, we applied the Drude extrapolation $R(\omega) \propto \omega^{-4}$.

B. Spectra of reflectivity and optical conductivity

In Fig. 3, we show reflectance spectra in $Y_{1-x}Ca_xVO_3$ at room temperature. In the insulating or semiconducting phase ($x \lesssim 0.4$), sharp structures due to optical phonons are observed in the infrared region, whereas the spectra are dominated by plasmalike photoresponse in the metallic phase ($x \gtrsim 0.6$). In particular, nine phonon modes are discernible in the end crystal YVO_3. The ob-

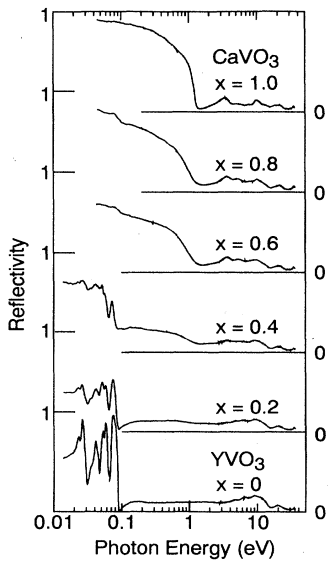

FIG. 3. Reflectance spectra of $Y_{1-x}Ca_xVO_3$ at room temperature.

served phonon structures are due to the lowered symmetry in the $GdFeO_3$-type lattice structure, since there would be only three infrared active modes in the ideal cubic (perovskitetype) structure. With carrier doping or with an increase of x, each phonon structure is gradually blurred, and the infrared high reflectance band comes out accompanying the reflectance edge around 1.1 eV.

Systematic spectral changes with x are also observed in the interband transition region above 3 eV. The changes are partly due to the mixed-crystal effect arising from differences in Y^{3+} and Ca^{2+} valence electron states. Fairly large changes below 8 eV are, however, mostly ascribed to the change in the filling of the $3d$ electron band and a resultant change in the $3d$ states near the Fermi level.

To see such a filling-dependent change in the $3d$ states, we show in Fig. 4 spectra of the optical conductivity $\sigma(\omega)$ below 7 eV in $Y_{1-x}Ca_xVO_3$ which were obtained by the aforementioned procedure of the Kramers-Kronig transformation. The spectral features shown in Fig. 4 are composed of two parts: (1) the intraband or Drude-like response of $3d$ states in the low-energy region (<3 eV), and (2) the interband transitions from O $2p$ bands to V $3d$ bands above 3 eV. The hole doping gradually increases the spectral weight in the infrared region, which seems to merge eventually into the Drude-like response, as typically seen in the spectrum of $CaVO_3$ ($x=1$). In accord with this, conspicuous changes are also seen for the spectra in the 3–7 eV region, which are perhaps due to the change of the final states (i.e., $3d$ electron bands) for the optical transitions, as discussed below.

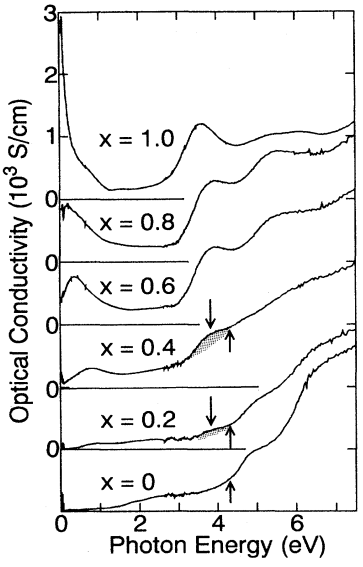

FIG. 4. Optical conductivity spectra of $Y_{1-x}Ca_xVO_3$ at room temperature. Upward arrows indicate the absorption edges of the CT excitations from O $2p$ to V $3d$ upper Hubbard bands. Hatched areas (indicated by downward arrows) correspond to CT transitions to the doping-induced states below the Mott-Hubbard gap (see text).

C. Electronic structures probed by optical spectra

1. Electronic structure in the parent insulator YVO_3

First, let us discuss the observed features in the parent Mott insulator YVO_3. As seen in the bottom spectrum of Fig. 4, $\sigma(\omega)$ shows a thresholdlike rise at 1.0–1.5 eV, apart from the structures due to optical phonons. The threshold photon energy is considered to correspond to the Mott-Hubbard gap. The rather blurred features of the gap excitation as well as the finite spectral weight even below 1.0 eV is partly due to a non-negligible concentration of hole-type carriers arising from the nonstoichiometry in the sample.

In the $\sigma(\omega)$ spectrum of YVO_3, we have further observed two absorption onset structures below 7 eV: around 4.3 (indicated by an upward arrow) and 5.6 eV. Judging from the energy positions and systematic changes with x *(vide infra)*, we have assigned these two absorption edges to the charge-transfer (CT) type transitions from the O $2p$ valence states to the t_{2g}- and e_g-like V $3d$ states, respectively, although Y $4d$-related transitions are also supposed to contribute to the spectra above 6 eV. The unoccupied t_{2g}-like state corresponds to the upper Hubbard band in this Mott insulator system. We show a schematic electronic structure in YVO_3 in Fig. 5(a). Relative energy positions of the O $2p$ and V $3d$ bands deduced from the present optical spectrum in YVO_3 are also indicated in Fig. 5(a) in units of eV. According to a recent photoemission study of YVO_3 (Ref. 14), the upper edge of the O $2p$ band lies approximately 3 eV lower than the upper edge of the $3d$ state. This energy separation is in accord with the observed energy difference between the Mott gap transition around 1.5 eV and the CT-type O $2p$–V $3d$ (upper Hubbard band) transition around 4.3 eV.

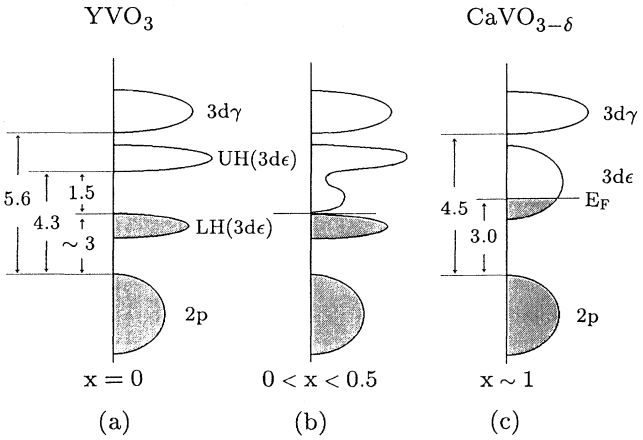

FIG. 5. Proposed models (schematic) for the density of states of O $2p$- and V $3d$-related states in $Y_{1-x}Ca_xVO_3$. Numbers in the figure represent the energy distances in units of eV.

2. *Change of infrared spectra with hole doping*

Let us proceed to the change in those spectra with hole doping. In the low-energy region, where only $3d$-like states are responsible for the transitions, we see a transition of the spectra from the gaplike feature in YVO_3 to the Drude-like one in $CaVO_3$. To see the change in more detail, we show in Fig. 6 the low-energy part of the conductivity spectra on a magnified scale. With hole doping, the spectral weight below 1.5 eV is critically increased. The onset of the optical conductivity is shifted to lower energy, showing a maximum in the midinfrared region at the intermediate doping levels, $x=0.2-0.6$. With further increasing x, such a midinfrared absorption tends to merge into the Drude-like absorption, as typically seen in the $x=1$ ($CaVO_3$) spectrum.

As a quantitative measure for the spectral weight, we have deduced the effective electron number ($N_{\rm eff}$) per V site by the following relation:

$$N_{\rm eff}(\omega)=\frac{2m_0V}{\pi e^2}\int_0^{\omega}\sigma(\omega')d\omega' \ .$$

Here, m_0 and V are the bare electron mass and cell volume containing one formular unit (one V site). $N_{\rm eff}(\omega)$ represents the number of electrons involved in the optical excitations up to the photon energy $\hbar\omega$. To estimate the spectral weight of the midinfrared band below the original Mott gap (~ 1.5 eV), we have taken the values of $N_{\rm eff}$ at 1.5 eV and plotted them in Fig. 7 against the concentration x of chemically doped holes. (The fixed point 1.5 eV is an appropriate, though not unique, energy scale for estimation of the spectral weight of the Drude-like contribution in the metallic phase.) Due to the existence of the Mott gap, $N_{\rm eff}$ (1.5 eV) for YVO_3 is small. $N_{\rm eff}$ increases continuously with x even for the nonmetallic region below $x_c\sim 0.5$, due to the contribution of the aforementioned midinfrared absorption below the Mott gap energy. A dashed straight line in Fig. 7 indicates a

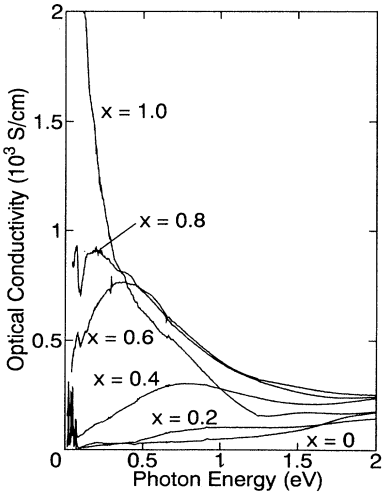

FIG. 6. Magnified spectra of the low-energy optical conductivity in $Y_{1-x}Ca_xVO_3$ at room temperature.

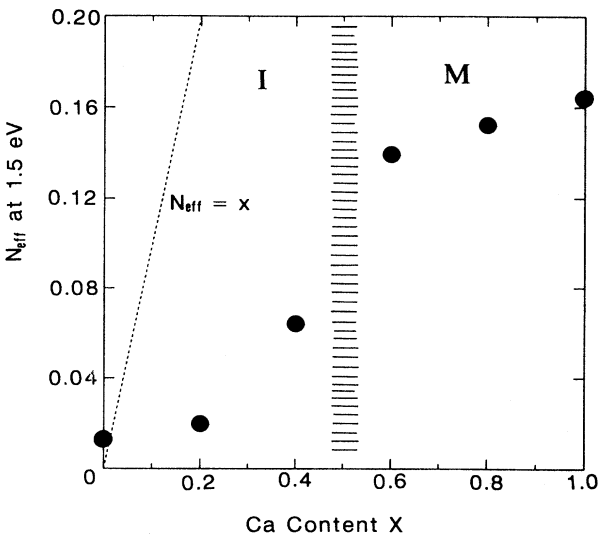

FIG. 7. The hole concentration (x) dependence of the effective number of electrons ($N_{\rm eff}$) at 1.5 eV in $Y_{1-x}Ca_xVO_3$. The hatched bar represents the metal(M)-insulator(I) phase boundary.

reference that $N_{\rm eff}=x$. The experimental points for the nonmetallic phase lie well below the line, indicating that the effective mass of the doped holes is strongly renormalized due to Coulombic interactions.

One may notice here that the observed transitional behavior in the infrared region for $Y_{1-x}Ca_xVO_3$ qualitatively resembles that observed in cuprate superconductors, for example in $La_{2-x}Sr_xCuO_4$ (Ref. 15) and $Pr_{2-x}Ce_xCuO_4$ (Ref. 16). Similarly, the layered cuprate compounds show the midinfrared absorption at relatively low doping levels, the maximum of which shifts to lower energy and eventually merges into the Drude-like tail with a further increase of x. Such a transitional behavior has been attributed to a reshuffling of the electronic structures and to the formation of the electronic states (so-called "in-gap" or "midgap" states) within the original CT gap with carrier doping. In layered cuprate compounds, the spectral weight for the midinfrared absorption arising from the in-gap state increases steeply as a function of the hole concentration x, e.g., $N_{\rm eff}$ (1.5 eV) $\gtrsim x$, and appears to be transferred from the CT excitations between the O $2p\sigma$- and Cu $3d$-like (upper Hubbard) bands.[13,14] In the case of $Y_{1-x}Ca_xVO_3$, however, the infrared spectral weight in the hole-doped sample appears to be transferred not only from the optical transitions between the original Hubbard bands, but also from the higher-lying CT transitions. This is perhaps because the energy position of O $2p$ states relative to V $3d$ bands becomes closer with x [*vide infra*; see also Fig. 5(c)] and hence shows a stronger hybridization between the $3d$ and $2p$ states in the higher-x samples.

3. *Change of the charge-transfer excitation bands*

Coming back to Fig. 4, one may also notice that the hole-doping procedure causes an appreciable change in

the interband transition region above 3 eV. For the $x=0.2$ compound, an additional transition is observed around 3.8 eV (indicated by a downward arrow in Fig. 4), just below the interband (O $2p$ to upper Hubbard band) transition edge (indicated by an upward arrow). The new band grows with further hole doping and eventually composes the main peak of the lower-lying (O $2p$–V $3d$ t_{2g}-like states) CT transition. In the $CaVO_3$ ($x=1$) sample, the optical conductivity shows the onsets at 3.0 and 4.5 eV (or the peaks around 3.5 and 5.0 eV), which can be assigned again to the CT bands from the O $2p$ valence states to the V $3d$ t_{2g}- and e_g-like states, respectively. Obviously, these transitions are shifted to lower energies by about 1.5 eV, as compared with the corresponding transitions in YVO_3. A schematic electronic structure in $CaVO_3$ is shown in Fig. 5(c).

One of the important features observed in intermediately hole-doped samples (e.g. $x=0.2$) and 0.4) is that the two distinct lower-lying CT excitations (O $2p$ to V t_{2g}-like $3d$ states) are discernible, as indicated by downward and upward arrows in the spectra of $x=0.2$ and 0.4 samples (Fig. 4). Since the initial state for the transitions is common, i.e., the topmost O $2p$ state, the double steps in the optical conductivity spectra represent a characteristic feature of density of states for the unoccupied $3d$ (t_{2g}-like) states in those hole-doped Mott insulators. In other words, the doping-induced new $3d$ states are formed near the Fermi level, which seems to coexist with the original upper Hubbard band [see Fig. 5(b)]. Such an in-gap state is likely also to be responsible for the midinfrared absorption band in the intermediately hole-doped compounds, as seen in Fig. 6. The upper Hubbard band as probed by the CT excitation spectra appears to almost collapse around $x=0.5$, where the insulator-metal transition takes place in the $Y_{1-x}Ca_xVO_3$ system.

V. SUMMARY

We have investigated a change of the optical conductivity spectra with varying of the $3d$ band filling in $Y_{1-x}Ca_xVO_3$ which can be viewed as a hole-doped Mott system. The insulator-metal transition takes place around $x=0.5$. With hole doping, the new electronic states are formed within the Mott-Hubbard gap and eventually replace the upper (and perhaps also lower) Hubbard band(s) to form the states near the Fermi level in the metallic composition region. Such in-gap states are also considered to be responsible for a midinfrared absorption peak. The transitional behavior of the midinfrared peak due to the in-gap states compares qualitatively with those observed in doped cuprate compounds, although there is a difference in the insulating nature, i.e. Mott type (YVO_3) vs CT type (layered cuprates). Such a remarkable reshuffling of the electronic structures over several eV around the Fermi level may be one of the most important features of the doping-induced insulator-metal transitions in strongly correlated electron systems.

Note added. After the first submission of this paper, it was reported by F. Iga and Y. Nishihara [J. Phys. Soc. Jpn. **61**, 1867 (1992)] that metallic (oxygen-deficient) $CaVO_3$ becomes insulating when oxygen deficiencies are filled by annealing the sample in air.

ACKNOWLEDGMENTS

The authors are grateful to A. Fujimori for enlightening discussion and to M. Fujisawa for his help in synchrotron radiation spectroscopy. This work was supported by Grant-In-Aids from Ministry of Education, Science and Culture, Japan.

*To whom correspondence should be addressed.

[1]For recent research activities, see, for example [Physica C **185-189** (1992)].

[2]J. Zaanen, G. A. Sawatzky, and J. W. Allen, Phys. Rev. Lett. **55**, 418 (1985).

[3]For a review, for example, J. M. Honig, in *The Metallic and Nonmetallic States of Matter,* edited by P. P. Edwards and C. N. R. Rao (Taylor and Francis, London, 1985), p. 261.

[4]See, for example, the review articles published in *The Metallic and Nonmetallic States of Matter,* edited by P. P. Edwards and C. N. R. Rao (Taylor and Francis, London, 1985).

[5]J. B. Torrance, P. Lacorre, A. I. Nazzal, E. J. Ansaldo, and Ch. Niedermayer, Phys. Rev. B **45**, 8209 (1992).

[6]For crystal structures and doping characteristics of cuprate superconductors, see, for example, Y. Tokura and T. Arima, Jpn. J. Appl. Phys. **29**, 2388 (1990).

[7]P. Dougier and A. Casalot, J. Solid State Chem. **2**, 396 (1970).

[8]P. Dougier and P. Hagenmuller, J. Solid State Chem. **15**, 158 (1975).

[9]M. Sayer, R. Chen, R. Fletcher, and A. Mansingh, J. Phys. C **8**, 2059 (1975).

[10]F. Deslandes, A. I. Nazzal, and J. B. Torrance, Physica C, **179**, 85 (1991).

[11]D. B. Rogers, A. Ferretti, D. H. Ridgley, R. J. Arnott, and J. B. Goodenough, J. Appl. Phys. **37**, 1431 (1966).

[12]P. Ganguly, Om. Parkash, and C. N. R. Rao, Phys. Status Solidi A **36**, 669 (1976).

[13]Y. Tokura and Y. Taguchi, in *Electronic Properties of High-Temperature Superconductors III,* edited by H. Kuzumany and J. Fink (Springer-Verlag, Berlin, 1992); Y. Taguchi and Y. Tokura (unpublished).

[14]H. Eisaki *et al.* (unpublished).

[15]S. Uchida, T. Ido, H. Takagi, T. Arima, Y. Tokura, and S. Tajima, Phys. Rev. B **43**, 7942 (1991).

[16]S. L. Cooper *et al.*, Phys. Rev. B **41**, 11 605 (1990).